

## 34. INTERSTITIAL WATER STUDIES ON SMALL CORE SAMPLES, LEG 11<sup>1</sup>

F. L. Sayles, Department of Chemistry, Woods Hole Oceanographic Institution, Woods Hole, Massachusetts,  
F. T. Manheim, U. S. Geological Survey, Woods Hole Oceanographic Institution, Woods Hole, Massachusetts, and  
L. S. Waterman, Department of Chemistry, Woods Hole Oceanographic Institution, Woods Hole, Massachusetts

### INTRODUCTION

The sediments cored at Sites 98, 99 and 100 are predominantly biogenic; those cored at Sites 101 through 106 are composed mainly of terrigenous material. As reported previously, most constituents in pore waters from the biogenic oozes exhibit minor changes in chemistry relative to sea water. In the terrigenous-hemipelagic sediments interstitial solutions initially of sea water composition have undergone considerable reaction. These reactions have produced large changes in the concentrations of calcium (Ca), magnesium (Mg), sulfate (SO<sub>4</sub>) and HCO<sub>3</sub> relative to sea water. In addition, this set of samples documents significant diagenetic alteration of sodium (Na) and chloride (Cl). Potassium exhibits little change in most samples, but in a few instances is depleted at depth.

The analytical techniques employed are identical to those described in earlier volumes of the *Initial Reports of the Deep Sea Drilling Project*. In an effort to identify alteration of sample composition during storage, salinity determinations<sup>2</sup> are made on the pore solution immediately upon their recovery from the sediments. The same measurement is made in the laboratory when the sample containers are opened for analysis. Occasionally evidence of evaporation is found as in Sample 104-2-5; the shipboard salinity was 32‰, while the laboratory measurement yielded 38‰. Changes of 3 to 4 per cent were also noted in several other samples as noted in the tables.

Adjustment of the analytically determined concentrations has been made and the corrected values presented in Tables 1 and 2. A large part of the work involved in the analyses of these samples has been done by Irene Uhlitzsch; we are indebted to her for the invaluable assistance she has rendered.

### RESULTS

The analytical data are summarized in Tables 1 and 2 (major and minor elements, respectively). The general trends observed in these analyses have, with the exception of changes in sodium and chloride, been noted on previous legs.

Chloride is depleted at most sites characterized by terrigenous-hemipelagic sediments; the concentration of chloride commonly decreases with depth to values of 18.4 to 18.6 gm/kg. At Site 104, chloride drops to 16.6 gm/kg, a value verified by triplicate analysis. Sodium is depleted in a number of samples from Sites 102 and 105. At the latter site, concentrations as low as 10.0 gm/kg are found. A few samples from Sites 101 and 104 also appear to exhibit depletion. Sodium enrichment occurs in some samples, most notably in several from Site 104.

In the terrigenous-hemipelagic sediments calcium depletions are characteristic of most pore water samples from Sites 102, 103, and 104. Calcium concentrations drop below our detection limit (0.01 gm/kg) in Sample 104-6-5. Samples from Sites 101 and 105 are enriched in calcium.

Sulfate and magnesium are strongly depleted in all of the interstitial solutions from terrigenous-hemipelagic sediments. Sulfate (SO<sub>4</sub>) concentrations in the pore fluids from many of the Leg 11 sites fall off to a few tenths of a gram per kilogram in the first forty meters of sediment (Sites 102, 103, 104 and 106). The depletions at Sites 101 and 105 are considerably smaller. Magnesium (Mg) concentrations decrease relatively smoothly with depth in most of these holes. Samples from the lower-most sediments commonly have magnesium concentrations in the range 0.3 to 0.4 gm/kg.

Alkalinity as measured in the samples from terrigenous-hemipelagic sediments exhibits both enrichment and depletion relative to sea water. Values almost an order of magnitude higher than that found in normal sea water have been measured (Sites 102 and 104). With the exception of Site 104, alkalinity appears to reach a maximum between 75 and 150 meters below the sea floor. In a number of instances, alkalinities well below

<sup>1</sup>Contribution No. 2729 of the Woods Hole Oceanographic Institution. Publication approved by the Director, U.S.G.S.

<sup>2</sup>Salinity has been determined by measuring the refractive index of the samples. These determinations are not more reliable than 0.5‰ as different instruments and personnel are used on the ship and in the laboratory.

TABLE 1  
Major Constituents of Pore Fluids. Values in g/kg (‰) Except as Noted

Sample Designation	Depth (m)	Age	Description	Na <sup>a</sup>	Na <sup>b</sup>	K	Ca	Mg	Total Cations (meq/kg)	Cl	SO <sub>4</sub>	Alk. (meq/kg)	HCO <sub>3</sub> <sup>c</sup>	Total Anions (meq/kg)	Sum <sup>d</sup>	Refractometer	H <sub>2</sub> O (%) <sup>e</sup>	pH
<b>Hole 98 (25°23.0'N, 77°18.7'W, water depth 2750 meters, Northeast Providence Channel)</b>																		
Surface ocean water				11.1	11.2 (11.0)	0.41 (0.41)	0.44 (0.43)	1.35 (1.35)	630 (621)	20.07	2.83	-	-	624	36.3	36.0	-	-
1-6	8	Lower Pliocene	Cream white foraminiferal-nannofossil ooze	10.8	10.8	0.43	0.43	1.28	608	19.51	2.59	3.9	0.24	607	35.3	35.1	30	7.5
3-5	24	Upper Miocene	Light gray foraminiferal-nannofossil ooze	10.8	11.0	0.48	0.46	1.23	614	19.71	2.40	-	-	605	35.3	36.1	37	7.3
4-6	63	Middle Miocene	Light greenish-gray foraminiferal-nannofossil ooze; mottled	11.0	11.0	0.47	0.49	1.20	613	19.69	2.57	4.1	0.25	612	35.7	35.5	30	7.5
5-3	94	Upper Oligocene	Light grayish-green to light olive gray foraminiferal-nannofossil ooze	11.0	11.1	0.48	0.49	1.25	622	19.87	2.63	3.9	0.24	618	36.1	36.2	34	7.4
6-6	138	Middle Eocene	Light greenish-white foraminiferal-nannofossil ooze	11.0	10.8	0.45	0.48	1.16	601	19.64	2.59	2.4	0.15	610	35.3	35.5	28	7.3
7-4	172	Middle to Lower Eocene	Pinkish white foraminiferal-nannofossil ooze	10.8	10.9	0.48	0.47	1.26	613	19.66	2.57	2.5	0.15	610	35.5	35.2	30	7.3
11-2	233	Upper to Middle Paleocene	Yellowish white foraminiferal-nannofossil ooze	10.8	10.8	0.51	0.45	1.31	613	19.80	2.67	-	-	613	35.5	35.8	25	7.1
<b>Hole 99A (23°41.2'N, 73°50.9'W, water depth 4922 m, S.E. of San Salvador)</b>																		
1-4	5	Lower Pleistocene	Brown foraminiferal-nannofossil ooze very clayey and silty	10.7	10.7	0.44	0.42	1.18	594	19.19	2.52	-	-	593	34.5	34.6	51	7.4
<b>Hole 100 (24°41.3'N, 73°48.0'W, water depth 5336 m)</b>																		
Surface ocean water				11.1	11.2 (11.0)	0.41 (0.42)	0.43 (0.43)	1.34 (1.34)	629 (620)	20.13	2.74	2.2	0.13	626	36.4	36.2	-	-
1-4	208	Valanginian-Tithonian (L. Cretaceous-Jurassi)	Greenish-gray nannofossil ooze with light gray banding throughout	10.7	10.6	0.35	0.98	1.09	608	20.01	2.37	1.3	0.08	614	35.5	35.5	21	7.2
<b>Hole 101 (25°11.9'N, 74°26.3'W, water depth 4773 m, southern end of Blake-Bahama Outer Ridge)</b>																		
Surface ocean water				11.1	11.2 (11.2)	0.41 (0.41)	0.43 (0.43)	1.35 (1.35)	630 (630)	20.12	2.78	-	-	626	36.4	36.3	-	-
1-5	38	Pliocene	Olive gray mottled hemipelagic clay with black pyrite specks and nodules	10.7	10.8 (10.7)	0.43 (0.43)	0.36 (0.36)	1.15 (1.16)	594 (590)	19.51	1.66	6.2	0.38	590	34.3	34.1	42	7.6
2-3	70	Late Miocene	Dark greenish-gray hemipelagic clay; olive gray mottling, pyrite	10.6	10.5	0.40	0.34	1.06	572	19.52	0.92	6.8	0.42	576	33.2	33.6	42	7.7
<b>Hole 101A (25°11.9'N, 74°26.3'W, water depth 4773 m, southern end of Blake-Bahama Outer Ridge)</b>																		
1-3	118	Late Middle Miocene	Dark greenish-gray hemipelagic clay; pyrite siderite, quartz, feldspar	10.7	10.8	0.38	0.40	1.04	585	19.71	0.96	7.3	0.44	582	33.7	33.6	33	7.7
2-5	162	Middle Miocene	Dark greenish-gray hemipelagic clay; siderite rutile, quartz common	10.4	10.6 (10.4)	0.37 (0.36)	0.43 (0.43)	0.94 (0.95)	569 (561)	19.66	0.17	4.0	0.24	561	32.4	32.4	33	7.7
3-2*	196	Middle Miocene	Dark greenish-gray hemipelagic clay; siderite and rutile common	9.97	9.97	0.34	0.43	0.94	541	18.49	0.94	-	-	541	31.1	33.0	33	7.6
<b>Hole 102 (30°43.6'N, 74°27.1'W, water depth 3414 m, crest of Blake-Bahama Outer Ridge)</b>																		
1-5	6	Pleistocene	Dark gray hemipelagic mud; black iron sulfide abundant	10.9	10.7 (10.7)	0.42 (0.42)	0.24 (0.23)	1.11 (1.11)	579 (579)	19.42	0.95	20.0	1.22	587	34.1	33.8	49	-
2-5	24	Pleistocene	Dark greenish-gray hemipelagic mud; specks of iron sulfide	10.4	10.7	4.41	0.10	1.02	564	19.42	0.19	-	-	551	31.8	33.0	45	7.8
4-4	101	Pleistocene	Olive gray hemipelagic mud; moderate mottling; nannofossils abundant	11.0	11.0	0.44	0.12	0.85	565	19.43	0.24	14.0	0.85	566	32.9	32.9	34	7.9

TABLE 1 – Continued

Sample Designation	Depth (m)	Age	Description	Na <sup>a</sup>	Na <sup>b</sup>	K	Ca	Mg	Total Cations (meq/kg)	Cl	SO <sub>4</sub>	Alk. (meq/kg)	HCO <sub>3</sub>	Total Anions (meq/kg)	Sum <sup>d</sup>	Refractometer	H <sub>2</sub> O (%) <sup>e</sup>	pH
5-5	139	Early Pleistocene	Greenish-gray hemipelagic mud	10.9	10.9 (10.8)	0.43 (0.43)	0.12 (0.12)	0.76 (0.76)	554 (550)	19.14	0.05	12.6	0.77	552	32.2	31.9	30	7.9
7-5	187	Early Pleistocene	Greenish-gray hemipelagic mud with varicolored mottling	10.9	10.6	0.43 (0.45)	0.16 (0.14)	0.70 (0.71)	538	19.10	0.05	10.9	0.66	550	31.7	-	34	8.1
10-3	309	Late Pliocene	Greenish-gray hemipelagic mud; mottled; nannofossils abundant	10.6	10.5	0.41	0.24	0.57	526	18.67	0.05	4.5	0.27	531	30.7	30.7	34	8.1
11-2*	355	Late Pliocene	Dark greenish-gray hemipelagic mud	10.3	10.2	0.44	0.23	0.50	555	18.15	0.05	0.7	0.04	512	30.7	30.0	28	8.1
12-4*	424	Middle Pliocene	Dark greenish-gray hemipelagic mud; nannofossils abundant	10.3	10.2	0.38	0.24	0.52	509	18.18	0.07	1.5	0.09	515	29.7	30.0	29	7.9
13-1	473	"Late-Early" Pliocene	Dark greenish-gray hemipelagic mud; nannofossils common; siderite common	10.5	10.4	0.35	0.34	0.57	525	18.48	0.33	0.8	0.05	528	30.5	30.7	30	7.8
17-1	618	Late Miocene	Dark greenish-gray indurated hemipelagic mud	11.1	11.2	0.34	0.52	0.76	584	19.24	1.53	3.6	0.22	578	33.8	33.0	29	7.4
18-3	637	Late Miocene	Dark greenish gray hemipelagic mud; lighter colored interbedding	10.6	10.7	0.33	0.49	0.37	528	18.42	0.29	0.6	0.04	526	30.6	30.2	23	7.8
19-1	660	Late Miocene	Dark greenish-gray hemipelagic mud; lighter colored irregular interbedding	10.8	10.6	0.23	0.51	0.44	528	18.59	0.46	4.7	0.29	538	31.1	30.8	27	7.4
<b>Hole 103 (30° 27.1'N, 74° 35.0'W, water depth 3992 m, S.W. flank of Blake-Bahama Outer Ridge)</b>																		
Surface ocean water				11.1	11.1	0.40	0.43	1.33	623	19.97	2.70	2.5	0.15	621	36.1	-	-	-
1-5	6	Early Pliocene	Green hemipelagic mud; firm layer	10.9	10.8	0.47	0.39	1.19	600	19.32	2.71	4.0	0.24	605	35.1	34.1	46	7.9
2-5	45	Late Miocene	Bluish-gray hemipelagic mud	10.7	10.6	0.42	0.17	0.81	547	19.24	0.09	7.2	0.44	551	31.8	31.6	38	7.8
3-3	97	Late Miocene	Dark greenish-gray hemipelagic mud; slight mottling	11.0	11.0	0.41	0.22	0.71	558	19.26	0.34	10.2	0.62	560	32.6	31.9	42	8.0
5-3	250	Late Middle Miocene	Dark greenish-gray hemipelagic mud; moderate mottling	11.2	11.0	0.41	0.11	0.43	529	18.71	0.34	1.8	0.11	536	31.1	30.8	28	7.9
<b>Hole 104 (30° 49.6'N, 74° 19.6'W, water depth 3833 m, N.E. flank of Blake-Bahama Outer Ridge)</b>																		
Surface ocean water				11.2	11.1	0.40	0.44	1.34	624	20.20	2.73 (2.63)	3.1	0.19	629	36.4	36.3	-	-
2-5*	42	Late Middle Miocene	Medium bluish-gray hemipelagic mud; moderate mottling of light bluish gray	11.6	11.6	0.47	0.02	0.81	583	20.13	0.17	14.3	0.87	585	34.1	32.2	41	7.5
3-4	67	Late Middle Miocene	Dark greenish-gray hemipelagic mud; slight mottling of lighter shades	11.3	11.2	0.46	0.04	0.66	555	19.08	0.19	17.2	1.05	559	32.7	31.9	57	7.6
4-5	139	Middle Miocene	Greenish-gray hemipelagic mud with dusky yellow mottling	11.4	11.3	0.49	0.01	0.47	543	18.56	0.15 (0.22)	21.1	1.29	547	32.3	31.4	47	8.0
6-5	225	Middle Miocene	Grayish-olive hemipelagic mud; slightly indurated layers abundant	10.4	10.3	0.44	<0.01	0.31	485	16.60	0.11	20.0	1.22	590	29.0	27.8	47	7.9
8-2	403	Middle Miocene	Grayish-olive hemipelagic mud interbedded with softer clay	11.7	11.6	0.44	0.06	0.29	542	18.40	0.31	21.5	1.31	546	32.4	31.1	38	7.8
<b>Hole 105 (34° 53.7'N, 69° 10.4'W, water depth 5245 m)</b>																		
2-2	33	Pleistocene or Middle Pliocene	Olive gray to greenish-gray hemipelagic mud	10.8	10.9	0.42	0.36	1.20	602	19.46	2.05 (2.17)	4.2	0.27	596	34.7	34.9	31	7.3
3-4*	96	Early Pliocene	Greenish-gray hemipelagic mud; slight mottling with lighter shades	10.3	10.6	0.35	0.36	1.08	575	18.91	1.44 (1.39)	-	-	563	32.7	33.3	34	7.4
8-4	273	Not Determined	Olive gray silty clay with light brown bands; heavy minerals common	10.0	10.2	0.26	0.67	0.97	563	18.92	1.09	-	-	556	32.1	32.2	27	7.3
13-3	325	Albian-Aptian	Green and black clay fragments tightly packed in soft greenish-black matrix	10.1	10.1	0.31	0.78	1.07	575	19.06	1.68	3.3	0.20	575	33.2	33.7	35	7.6

TABLE 1 – Continued

Sample Designation	Depth (m)	Age	Description	Na <sup>a</sup>	Na <sup>b</sup>	K	Ca	Mg	Total Cations (meq/kg)	Cl	SO <sub>4</sub>	Alk. (meq/kg)	HCO <sub>3</sub> (meq/kg)	Total Anions	Sum <sup>d</sup>	Refractometer	H <sub>2</sub> O (%) <sup>e</sup>	pH
<b>Hole 106 (36°26.0'N, 69°27.7'W, water depth 4492 m)</b>																		
Surface ocean water				11.0	11.2	0.41	0.43	1.34	630	20.08	2.58	2.9	0.18	622	36.2	36.2	-	-
1-2	2	Quaternary	Olive gray hemipelagic mud admixed and interlayered with reddish brown	11.1	10.8	0.44	0.41	1.22	588	19.29	2.58	4.4	0.27	602	35.0	35.1	47	7.5
3-4*	115	Early Pleistocene	Light brownish-gray hemipelagic mud	10.3	10.6	0.34	0.19	0.77	555	18.97	0.13 (0.16)	5.0	0.30	542	31.3	31.1	28	8.0

\*Note: Values corrected for evaporation occurring during storage as determined by refractive index measurement before and after storage.

<sup>a</sup>Sodium determined by differences between anions and cations excluding Na.

<sup>b</sup>Sodium determined directly. Values in parentheses refer to separate samples carried through the entire sampling and analytical processes. The total cation values shown are determined using these values and means of duplicate determinations, where available.

<sup>c</sup>HCO<sub>3</sub> is calculated from total alkalinity, assuming this is entirely due to bicarbonate ion.

<sup>d</sup>The sum incorporates the calculated Na values and means of replicate value where available. Minor constituents are not included but with the exception of strontium in some samples contribute less than 0.1% to the sum.

<sup>e</sup>pH and water content are taken from shipboard summaries.

**Table 2**  
**Minor Constituents. Concentrations in mg/kg (ppm). (a) Colorimetric Determination; (b) Emission Spectrographic Determination**

Sample Designation	Depth (m)	Age	Description	Sr	Ba	Si (col.)	Si (spec.)
<b>Hole 98</b>							
Surface ocean water				10	<0.1	1	<5
1-6	8	Lower Pliocene	Cream white foraminiferal-nannofossil ooze	23	<0.1	6	<5
3-5	24	Upper Miocene	Light gray foraminiferal-nannofossil ooze	52	<0.1	6	<5
4-6	63	Middle Miocene	Light greenish-gray foraminiferal-nannofossil ooze; mottled	48	<0.1	8	9
5-3	94	Upper Oligocene	Light grayish-green to light olive gray foraminiferal-nannofossil	47	0.2	14	13
6-6	138	Middle Eocene	Light greenish-white foraminiferal-nannofossil ooze	39	0.2	12	23
7-4	172	Middle to Lower Eocene	Pinkish white foraminiferal-nannofossil ooze	42	0.2	11	18
11-2	233	Upper to Middle Paleocene	Yellowish white foraminiferal-nannofossil ooze	—	—	—	—
<b>Hole 99A</b>							
1-4	5	Lower Pleistocene	Brown foraminiferal-nannofossil ooze very clayey and silty	10	<0.1	—	<5
<b>Hole 100</b>							
Surface ocean water				12	<0.1	—	<5
1-4	208	Valanginian-Tithonian	Greenish-gray nannofossil ooze with light gray banding throughout	19	0.2	—	<5
<b>Hole 101</b>							
Surface ocean water				10	<0.1	—	<5
1-5	38	Pliocene	Olive gray mottled hemipelagic clay with black pyrite specks and nodules	—	—	<1	—
2-3	70	Late Miocene Miocene	Dark greenish-gray hemipelagic clay; olive gray mottling, pyrite	13	0.3	3	<5
<b>Hole 101A</b>							
1-3	118	Late Middle	Dark greenish-gray hemipelagic clay; pyrite, siderite, quartz, feldspar	12	0.7	10	13
2-5	162	Middle Miocene	Dark greenish-gray hemipelagic clay; siderite and rutile common	16	1.3	10	5
3-2	196	Middle Miocene	Dark greenish-gray hemipelagic clay; siderite, rutile, quartz common	—	—	<1	—
<b>Hole 102</b>							
1-5	6	Pleistocene	Dark gray hemipelagic mud; black iron sulfide abundant	10	0.2	14	14
2-5	24	Pleistocene	Dark greenish-gray hemipelagic mud; specks of iron sulfide	9	5.0	—	<5

TABLE 2 — Continued

Sample Designation	Depth (m)	Age	Description	Sr	Ba	Si (col.)	Si (spec.)
4-4	101	Pleistocene	Olive gray hemipelagic mud; moderate mottling; nannofossils abundant	—	—	11	—
5-5	139	Early Pleistocene	Greenish-gray hemipelagic mud	10	>6.0	17	17
7-5	187	Early Pleistocene	Greenish-gray hemipelagic mud with vari-colored mottling	11	>6.0	11	8
10-3	309	Late Pliocene	Greenish-gray hemipelagic mud; mottled; nannofossils abundant	15	8.0	10	12
11-2*	355	Late Pliocene	Dark greenish-gray hemipelagic mud	13	5.0	9	8
12-4*	424	Middle Pliocene	Dark greenish-gray hemipelagic mud; nannofossils abundant	15	4.0	9	7
13-1	473	“Late-Early” Pliocene	Dark greenish-gray hemipelagic mud; nannofossils common; siderite common	16	4.0	7	14
17-1	618	Late Miocene	Dark greenish-gray indurated hemipelagic mud	16	0.4	9	18
18-3	637	Late Miocene	Dark greenish-gray hemipelagic mud; lighter colored interbedding	17	4.0	6	<5
19-1	660	Late Miocene	Dark greenish-gray hemipelagic mud; lighter colored irregular interbedding	15	1.1	—	<5
<b>Hole 103</b>							
Surface ocean water				13	0.1	<1	<5
1-5	6	Early Pliocene	Green hemipelagic mud; firm layer	9	0.1	—	<5
2-5	45	Late Miocene	Bluish-gray hemipelagic mud	14	0.9	5	13
3-3	97	Late Miocene	Dark greenish-gray hemipelagic mud; slight mottling	11	2.0	11	12
5-3	250	Late Middle Miocene	Dark greenish-gray hemipelagic mud; moderate mottling	12	4.0	4	<5
<b>Hole 104</b>							
Surface ocean water				10	<0.1	—	<5
2-5*	42	Late Middle Miocene	Medium bluish-gray hemipelagic mud; moderate mottling of light bluish gray	12	3.0	7	<5
3-4	67	Late Middle Miocene	Dark greenish-gray hemipelagic mud; slight mottling of lighter shades	15	5.0	—	26
4-5	139	Middle Miocene	Greenish-gray hemipelagic mud with dusky yellow mottling	15	5.0	19	<5
6-5	225	Middle Miocene	Grayish-olive hemipelagic mud; slightly indurated layers abundant	16	6.0	21	23
8-2	403	Middle Miocene	Grayish-olive hemipelagic mud interbedded with softer clay	11	2.0	14	8
<b>Hole 105</b>							
2-2	33	Pleistocene or Middle Pliocene	Olive gray to greenish-gray hemipelagic mud	10	0.3	7	<5
3-4*	96	Early Pliocene	Greenish-gray hemipelagic mud; slight mottling with lighter shades	12	0.3	—	<5
8-4	273	Not Determined	Olive gray silty clay with light brown bands; heavy minerals common	—	—	—	—
13-3	325	Albian-Aptian	Green and black clay fragments tightly packed in soft greenish-black matrix	20	0.4	5	13

TABLE 2 — Continued

Sample Designation	Depth (m)	Age	Description	Sr	Ba	Si (col.)	Si (spec.)
<b>Hole 106</b>							
Surface ocean water				12	<0.1	—	<5
1-2	2	Quaternary	Olive gray hemipelagic mud admixed and interlayered with reddish brown	11	0.1	—	15
3-4*	115	Early Pleistocene	Light brownish-gray hemipelagic mud	7	0.3	—	<5

\*Note: Values corrected for evaporation occurring during storage as determined by refractive index measurement before and after storage.

normal values for sea water are reported; these low values are invariably found in samples from the deeper portion of the drill holes.

Changes in potassium (K) relative to sea water are small in the terrigenous-hemipelagic sediments. In most cases the enrichments observed are of a size attributable to temperature effects (Mangelsdorf *et al.*, 1969; Bischoff *et al.*, 1970). Our lack of knowledge of the changes in exchange equilibria as a function of temperature coupled with very incomplete knowledge of thermal gradients in these thick sediments preclude accurate assessment of the significance of the observed enrichments. The high concentrations at Site 104 and in Samples 102-7-5, 102-10-3 and 102-11-2 do appear to represent significant enrichment; the rest are questionable.

Of the minor constituents in the pore fluids from the nonbiogenic sediments, barium (Ba) fluctuates most widely. Characteristic of sediments in which sulfate has been depleted, barium is strongly enriched to concentrations of 2 to 5 ppm. Silica (Si) concentrations generally range from 5 to 20 ppm. There are an abnormally large number of low silica values (<6 ppm).

The interstitial water samples from the biogenic sediments (Sites 98, 99 and 100) are characterized by only minor deviations from sea water. Potassium exhibits significant enrichment at Site 98, as does calcium. Alkalinity is slightly high (4.1 meq). As commonly observed, strontium (Sr) is enriched some four- to six-fold. Silica concentrations are relatively low, particularly in the upper part of Site 98.

The accuracy of the major element analyses, as represented by analyses of three Copenhagen sea water samples stored and treated in the same fashion as the samples here, is as follows: Na, 0.6% low; Mg, 0.6% low; Ca, 0.5% high; K, 0.1% high; Cl, 0.5% low (6 samples); SO<sub>4</sub>, 1.1% low. The precision for the major elements based upon replicate analyses is Na, ±1%; K, ±1%; Ca, ±0.5%; Mg, ±0.5%; Cl, ±0.3%; SO<sub>4</sub>, ±1.7%; HCO<sub>3</sub>, ±7%. The minor element data (Table 2) for this leg suffer from technical problems in the emission spectrographic analysis. These data are not as accurate as the data of previous legs. They should be considered as semi-quantitative in nature.

## DISCUSSION

The minor chemical alteration of pore fluids found in the biogenic sediments of Leg 11 is characteristic of calcareous deposits throughout the world ocean. Discussion of these changes is presented in reports for Legs 6 through 9. The silica concentrations at Site 98 are relatively low in the samples from Cores 1 to 4 as compared to most biogenic sediments. This reflects the paucity of siliceous skeletal debris and control of silica concentration by silicate minerals. The increases in

silica in the samples from Cores 5 and below are a response to the increased content of amorphous SiO<sub>2</sub> and virtual absence of silicate minerals in these sediments. The potassium enrichment at Site 98 is also atypical of most biogenic sediments; constancy or slight depletion is normally observed. Volcanic glass has been reported in some samples from this site but it is rare. The enrichment could be due to dissolution of the glass combined with the complete absence of clays and micas (below Core 6) which characteristically take up potassium.

Depletion of sodium in the interstitial solutions of terrigenous-hemipelagic sediments is well-documented at several sites. The samples from Site 105 exhibit this loss most clearly, but the low sodium concentrations recorded at Sites 102 and 104 are significant. The relatively high sodium concentrations, particularly at Site 104, are also significant.

The loss of sodium is difficult to explain. Reactions between rock forming minerals common to argillaceous sediments can be expected to release sodium into solution. The sediments at Sites 102 through 106 are composed of from 10 to 60 per cent montmorillonite (Zemmels *et al.*, 1971). Whitehouse and McCarter (1958) have shown that montmorillonite will react with sea water at low temperatures and pressures. The solids in the latter experiments lost sodium while gaining potassium and magnesium. Numerous studies of clay mineral diagenesis (see Dunoyer de Segonzac, 1970, and references therein) have demonstrated that as temperature and pressure increase on burial, montmorillonite reacts to yield mixed-layer clays. These changes all favor magnesium and potassium uptake over that of sodium in the reaction products. The location of the Leg 11 sites is such that dilution by fresh water is not reasonable nor does the Na-Cl relationship indicate that such an explanation is plausible (see Figure 1a). At this time we have no definite answer to the question of what reactions lead to the depletion of sodium.

It is evident from the foregoing discussion that enrichment of the interstitial solutions with sodium would be expected during burial. The generally high sodium concentrations at Sites 103 and 104 could reflect the earliest stages of clay mineral diagenesis. Alternatively, the uptake of magnesium and release of sodium may be due to montmorillonite formation from such minerals as plagioclase or potassium feldspar, or possible volcanic glass.

Small but significant depletions of chloride characterize many of the samples from Sites 102, 104, and 105. There appears to be a rough depth control in that only samples from below 75 to 150 meters exhibit readily discernible chloride depletion. As the chloride ion is only a trace component of common minerals,

few reactions can be cited to explain the observed losses.

A rather strong correlation is found between magnesium and chloride, especially if only those samples from depths of 100 meters or more are considered (see Figure 1b). An interpretation of this correlation is difficult to put forward; the correlation may be coincidental. Both magnesium and chloride vary with depth and the correspondence could arise from temperature or pressure effects on independent reactions. As in the case of sodium, no mechanistic interpretation of the chloride depletion is readily apparent.

In many of the samples from Leg 11, magnesium and sulfate depletions correlate linearly (Figure 1c). There is considerable deviation from this correlation at very low sulfate ( $\text{SO}_4$ ) concentrations, however, indicating that loss of magnesium from interstitial solution continues after sulfate is essentially exhausted. Drever (1971) has demonstrated the uptake of nonexchangeable magnesium by clays under reducing conditions in near-surface sediments. He has suggested that the formation of pyrite through sulfate reduction has led to the replacement of iron (Fe) in montmorillonites by magnesium. Drever has utilized pore fluid data from earlier Initial Reports to demonstrate a correlation such as that exhibited by the data presented in Figure 1c; this reaction best explains the Mg- $\text{SO}_4$  correlation. Drever's data from the Rio Ameco demonstrate that the replacement of iron by magnesium in montmorillonites is a relatively rapid reaction occurring in near-surface sediments where sulfate reduction has occurred. The continued loss of magnesium after the virtual exhaustion of sulfate is indicative of other processes. This loss may reflect the alteration of clays in the sediment, dolomite formation, or weathering of components in these terrigenous-hemipelagic sediments.

The data from Table 1 demonstrate that magnesium uptake occurs at depths in the sediment of less than 100 meters. Data from earlier legs show that uptake at these depths is common in terrigenous-hemipelagic sediments. Published data on variations in clay mineralogy with burial depth indicate, however, that changes in clay mineral structures are detectable only at depths far in excess of 100 meters. For instance, Burst (1959, 1969) has demonstrated a decrease in montmorillonite in Eocene sediments of the Gulf Coast that is detectable only below approximately 1000 meters. He has attributed the decrease to recrystallization and noted that below this depth the montmorillonite mixed-layering increased with increasing depth. Numerous other studies have indicated similar depth control (see Dunoyer de Segonzac, 1970). On the other hand, experimental data have demonstrated that alteration of montmorillonite in sea water may proceed at

low temperatures and pressures (Whitehouse and McCarter, 1958). However, these experiments have shown that the alteration of the montmorillonite is characterized by both magnesium and potassium uptake by the solids. The Leg 11 data demonstrate that magnesium losses occur, but only rarely are potassium losses recorded. The absence of detectable crystallographic alteration of montmorillonite at shallow depth indicates that if such reactions occur, they must be limited to only the earliest stages of change. The absence of potassium depletion from the Leg 11 samples suggests that in these sediments no alteration of montmorillonite to mixed-layer types of clay has occurred. It should be noted, however, that data from numerous earlier legs has demonstrated that the concurrent uptake of magnesium and potassium from interstitial solution at shallow depths in the sediment is not uncommon. Such data are compatible with the incipient alteration of montmorillonite at low temperatures and pressures as suggested by the experiments of Whitehouse and McCarter (1968).

Drever (1971) has suggested that the depletion of magnesium in pore fluids not attributable to the Mg-Fe- $\text{SO}_4$  reaction noted above is due to the formation of dolomite. The data from Leg 11 do not provide evidence in support of this mechanism of magnesium removal. X-ray diffraction data (Zemmels *et al.*, 1971) demonstrate that there is no correlation between magnesium loss and the presence or absence of dolomite in these sediments. Further, the loss of calcium is inadequate to explain the depletion of magnesium in excess of that utilized in the Mg-Fe- $\text{SO}_4$  reaction if dolomite stoichiometry is maintained. The loss of magnesium over and above that attributable to the Mg-Fe- $\text{SO}_4$  reaction may be calculated from the total magnesium depletion (relative to sea water) and the Mg- $\text{SO}_4$  correlation of Figure 1c. When the "excess" magnesium loss is compared to the total calcium depletion, it is readily apparent that, on a mole to mole basis, the "excess" magnesium loss is two to ten times the total calcium loss. Such proportions cannot be indicative of dolomite formation. Additional calcium could be supplied through solid phase dissolution, but there is no direct evidence of dolomite precipitation correlating with magnesium losses from the interstitial solutions.

Without information from the solids, explanation of the magnesium losses must remain speculative. Of the alternatives available, weathering of silicates common to terrigenous-hemipelagic sediments appears to provide the best fit to our data. The alteration of plagioclase or potassium feldspars to montmorillonite would lead to magnesium depletion and, depending on the reactant, possibly to potassium enrichment in the pore fluids. The sodium enrichments observed in these solutions are qualitatively in agreement with such reactions also.

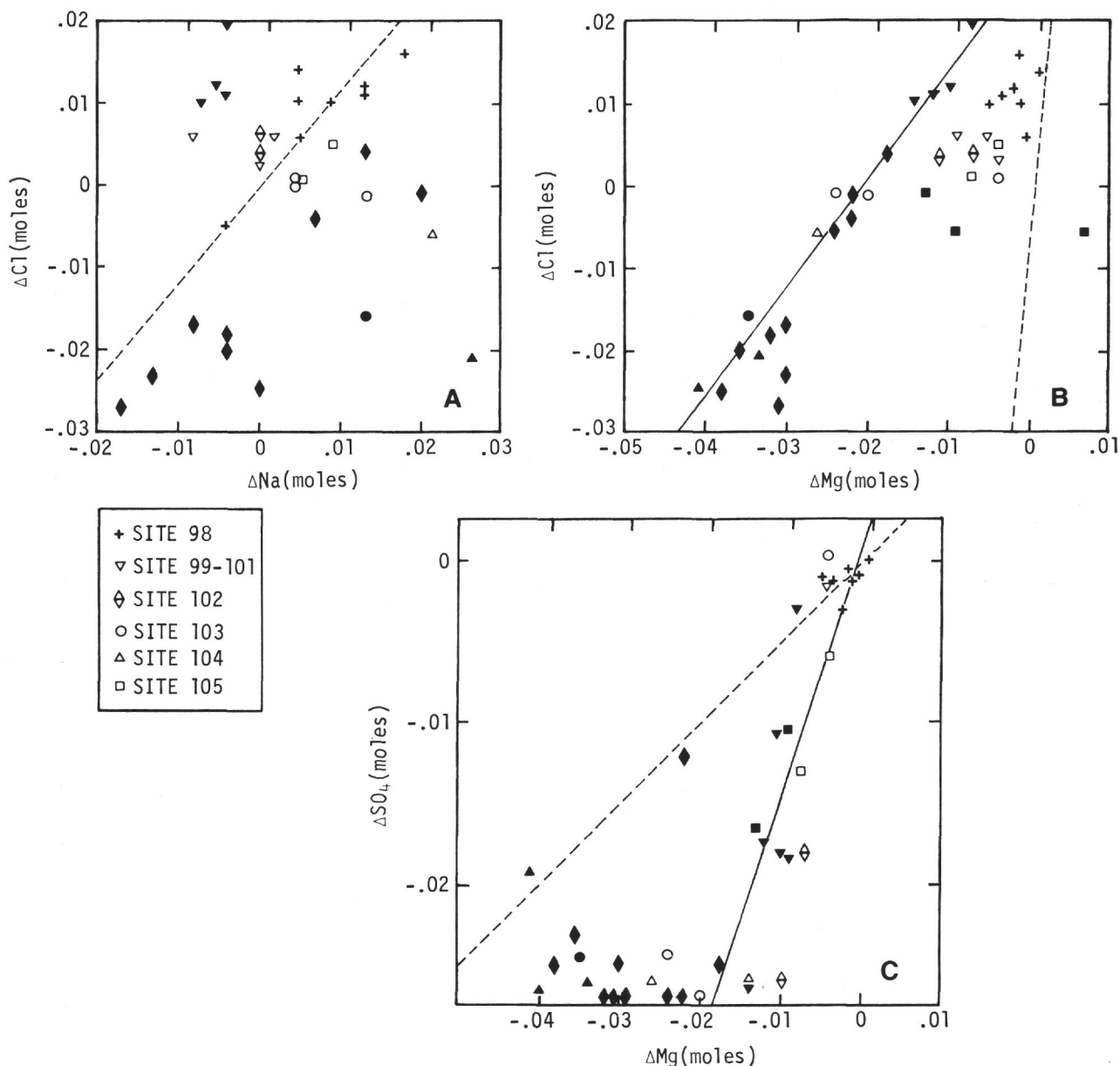


Figure 1. Co-variation of various constituents of the pore fluids. The notation used is the change in concentration (molar) as calculated by subtracting the concentration in standard sea water with a salinity of 35.0‰ from the analytical value. Losses are denoted as negative. The dashed lines represent the theoretical variation of concentration due to either dilution or evaporation. The solid symbols are samples from depths in excess of 100 meters; the open symbols represent shallower samples. The solid line in Figure 1B is a least squares fit for all data points from subbottom depths of 100 meters or more. The solid line in Figure 1C is a least squares fit of all data points with sulfate losses not in excess of 0.022 moles.

In samples analyzed from Leg 15 it was noted that where the alkalinity is very high, measurements made on board ship yielded systematically higher results than did those carried out on stored samples. It appears that carbon-dioxide loss from these samples has occurred. To alter the alkalinity carbon-dioxide loss must be accompanied by calcium-carbonate precipitation. The

correspondence between calcium and  $HCO_3$  is presented in Figure 2. Most samples are supersaturated with respect to calcite at a pH of 8, many are at or slightly above saturation at a pH of 7.6. The calculations have been carried out for the temperature at which the samples were stored (4°C). The pH values of 7.6 and 8.0 are the range into which most samples

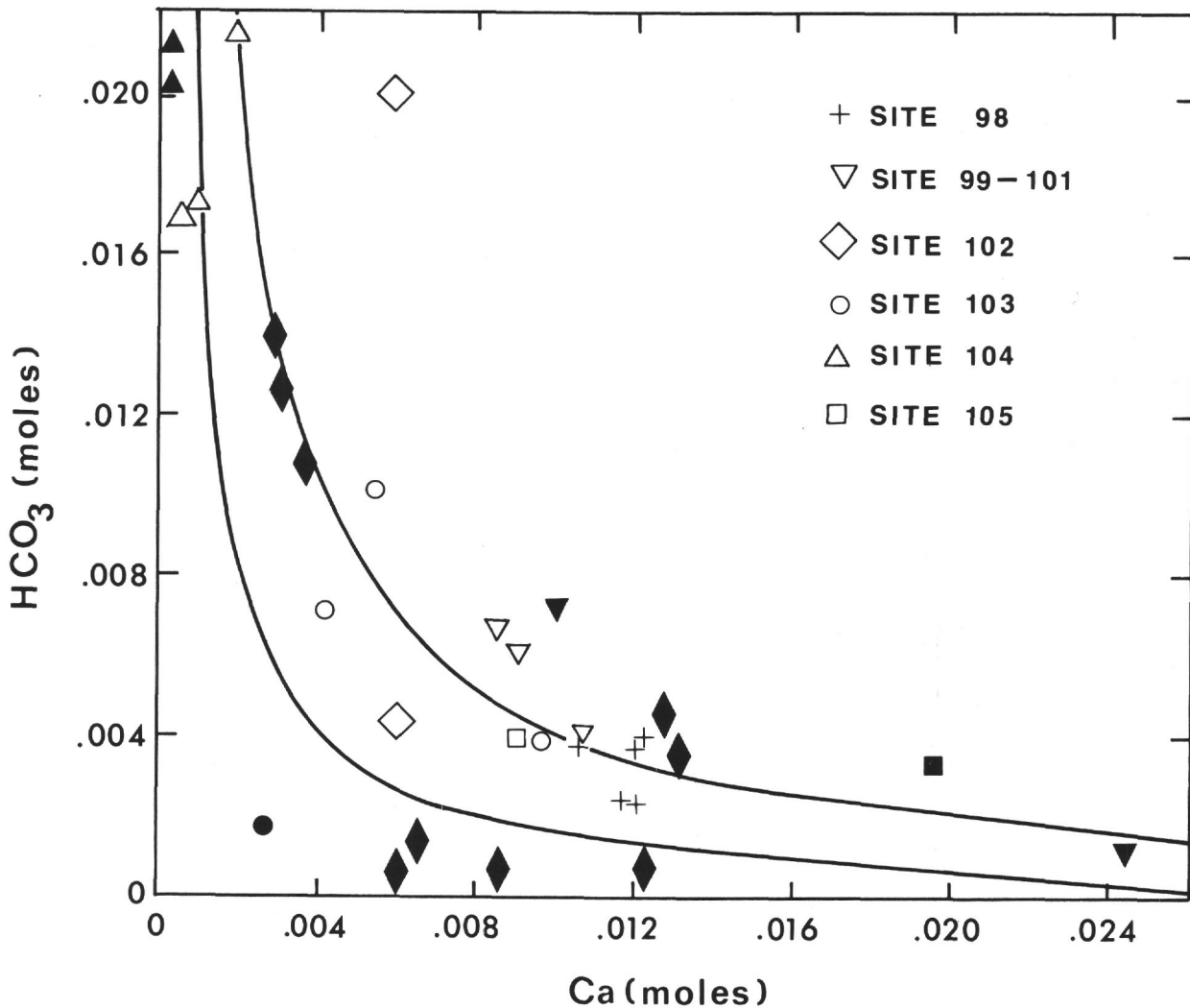


Figure 2. Co-variation of  $\text{HCO}_3^-$  and Ca. The solid curves represent saturation with respect to calcite at the indicated pH at  $4^\circ\text{C}$  (see text). Open and solid symbols represent samples from sediment depths of less than 100 meters and depths equal to or greater than 100 meters, respectively.

fall.<sup>1</sup> Figure 2 demonstrates that precipitation of calcium carbonate is possible in most samples. On the basis of the latter and on the Leg 15 results, precipitation is limited to samples whose alkalinities are well above that of surface sea water. The alkalinity loss may amount to 25 per cent. Such changes will produce detectable errors in the calcium concentration.

Until further quantitative assessment of the precipitation of calcium carbonate during storage is made, the

<sup>1</sup>It can be argued that curves representing saturation with respect to aragonite rather than calcite would be more appropriate. Such a change would shift the curves only slightly. The effect is not important for our purposes.

calcium values must be considered suspect. We estimate that the errors are small for they affect primarily those samples with very high alkalinity. In these samples the slope of the saturation curve is steep and changes of  $\text{HCO}_3^-$  will lead to small absolute changes in calcium concentration. The errors do not obscure the basic relationship between calcium and  $\text{HCO}_3^-$  which is indicative of equilibria with crystalline calcium carbonate. This is an *in situ* feature and not an artifact.

The minor element trends are much the same as has been observed previously. The silica concentrations are relatively low in most samples. This is a reflection of control of silica by silicate mineral solubility (Site 105, upper portion of Sites 98 and 103). Where more than a

trace of amorphous silica is found, the concentration of silica increases to levels reflecting amorphous silica solubility (the lower portion of Site 98 and from 67 meters to the bottom of Site 104). Barium reflects the redox state of the sediments being indirectly controlled by the redox state through barium-sulfate equilibria and sulfate reduction.

All of the chemical reactions, discussed above, involving the constituents of the interstitial solutions lead to the establishment of chemical gradients within the sediments. All of the elements exhibit gradients at many of the sites. In preceding Initial Reports we have noted that diffusive communication in sediments, at least vertically, is good (cf. Legs 1, 7, 9 and 10 Initial Reports). The existence of strong chemical gradients at the Leg 11 sites demonstrates that the reactions producing them are proceeding at the present time. These are not early stage diagenetic reactions limited to the near-surface sediments. The existence of coherent trends through as much as 600 meters of sediment suggests that, commonly, the same reactions occur over the entire interval. Only the reactions involving exhaustible components (such as  $\text{SO}_4$  and  $\text{O}_2$  from sea water) are limited to the upper few tens of meters of sediment. Further, the rates of reaction must be rapid relative to diffusive readjustment. Were this not the case, smooth gradients, or the absence of gradients, would characterize the variation in interstitial solution composition with depth (cf. Legs 7 and 9 Initial Reports).

## REFERENCES

- Bischoff, J. L., Greer, R. E. and Luistro, A. O., 1970. Composition of interstitial waters of marine sediments: temperature of squeezing effect. *Science*. **167**, 1245.
- Burst, J. F., 1959. Postdiagenetic clay-mineral environmental relationship in the Gulf Coast Eocene. *Proc. Nat. Conf. Clays and Clay Minerals*. 6th, Nat. Acad. Sci. Nat. Res. Council, 327.
- , 1969. Diagenesis of Gulf Coast clayey sediments, and its possible relation to petroleum migration. *Bull. Am. Assoc. Petrol. Geologists*. **53**, 73.
- Drever, J. I., 1971. Magnesium-iron replacement in clay minerals in anoxic marine sediments. *Science*. **172**, 1334.
- Dunoyer de Segonzac, G., 1970. The transformation of clay minerals during diagenesis and low grade metamorphism; a review. *Sedimentology*. **15**, 281.
- Mangelsdorf, P. C., Jr., Wilson, T. R. S. and Daniell, E., 1969. Potassium enrichments in interstitial waters of recent marine sediments. *Science*. **165**, 171.
- Whitehouse, Grant, U. and McCarter, R. S., 1958. Diagenetic modification of clay mineral types in artificial sea water. *Proc. Nat. Conf. Clays and Clay Minerals*. 5th, Nat. Acad. Sci. Nat. Res. Council, Publ. 556, 81.
- Zemmels, I., Cook, H. E., and Hathaway, J. C., 1971. X-ray mineralogy studies – Leg 11. In Ewing, J. I. et al., 1971. *Initial Reports of the Deep Sea Drilling Project, Volume XI*. Washington (U. S. Government Printing Office), this volume.